Sunshape measurements with conventional rotating shadowband irradiometers

Stefan Wilbert, Marc Röger, Jonas Csambor, Moritz Breitbach, Florian Klinger, Bijan Nouri, Natalie Hanrieder, Fabian Wolfertstetter, David Schüler, S. Shaswattam, Neeraj Goswami, Sharad Kumar, Abdellatif Ghennioui, Roman Affolter, Norbert Geuder, and Birk Kraas

Citation: AIP Conference Proceedings **2033**, 190016 (2018); doi: 10.1063/1.5067201

View online: https://doi.org/10.1063/1.5067201

View Table of Contents: http://aip.scitation.org/toc/apc/2033/1

Published by the American Institute of Physics

Sunshape Measurements with Conventional Rotating Shadowband Irradiometers

Stefan Wilbert[1a)], Marc Röger[1], Jonas Csambor[2], Moritz Breitbach[3], Florian Klinger[1], Bijan Nouri[1], Natalie Hanrieder[1], Fabian Wolfertstetter[1], David Schüler[4], S. Shaswattam[5], Neeraj Goswami[5], Sharad Kumar[5], Abdellatif Ghennioui[6], Roman Affolter[3], Norbert Geuder[7], Birk Kraas[8]

[1]*German Aerospace Center (DLR), Institute of Solar Research, Ctra. de Senés s/n km 5, 04200 Tabernas, Spain.*
[2]*Universität Stuttgart, Keplerstraße 7, 70174 Stuttgart, Germany.*
[3]*CSP Services. Paseo de Almería 73, 2, 04001 Almería, Spain.*
[4]*RV realtime visions GmbH, Ferdinand-Sauerbruch-Straße 25-33, 56073 Koblenz, Germany.*
[5]*NETRA, NTPC Ltd., E3 Echotech Ii, Udhyog Vihar Greater Noida, Gautam Budh Nagar. Pin 201306 Up-India.*
[6]*Institut de Recherche en Energie Solaire et Energies Nouvelles IRESEN, Green Energy Park Benguerir, Morocco.*
[7]*Prof. Dr., Hochschule für Technik Stuttgart, Schellingstrasse 24, 70174 Stuttgart, Germany*
[8]*CSP Services GmbH, Friedrich-Ebert-Ufer 30, 51143 Cologne, Germany.*

[a)]Corresponding author: Stefan.wilbert@dlr.de

Abstract. Because of forward scattered radiation in the atmosphere, the circumsolar region closely surrounding the solar disk looks very bright. The radiation coming from this region, the circumsolar radiation, is in large part included in direct normal irradiance (DNI) measurements at the usual 2.5° pyrheliometer opening half angle, but only partially intercepted by the receivers of focusing solar collectors. Therefore, circumsolar radiation measurements are recommended to be included in solar resource assessment. Circumsolar radiation can be characterized using the radial angular distribution of the radiance around the center of the sun – the so-called sunshape. Several sunshape measurement methods have been developed recently. Most approaches use cameras or pyrheliometers with different apertures which require daily maintenance. The Rotating Shadowband Irradiometer (RSI) based method discussed here uses a conventional RSI without any hardware modification to enable sunshape measurements without affecting the RSI's fundamental function as a DNI measurement device. Thus, it allows to measure circumsolar radiation without any additional hardware and with significantly lower maintenance requirements. The presented RSI-based sunshape measurement algorithm has been validated with four RSIs and more than two years of data. After a short description of the method to derive the circumsolar contribution, the validation results are shown. Then the required calibration method is discussed, followed by the results from the measurement campaigns at four sites in Spain, India and Morocco. It was found that no individual calibration is required per instrument and the algorithm can be used for automatic data processing so that common RSI stations can measure the sunshape with comparably low extra effort. Furthermore, we explain how to derive sunshapes from the RSI measurements.

INTRODUCTION

Due to forward scattering of direct sunlight in the atmosphere, the circumsolar region closely surrounding the solar disk looks very bright. The radiation coming from this region, the circumsolar radiation, is in large part included in direct normal irradiance (DNI) measurements at the usual 2.5° pyrheliometer opening half angle, but only partially intercepted by the receivers of focusing solar collectors. Hence, circumsolar radiation measurements are recommended to be included in solar resource assessment as explained in detail in [1]. Circumsolar radiation can be characterized using the radial angular distribution of the radiance around the center of the sun – the so-called

SolarPACES 2017
AIP Conf. Proc. 2033, 190016-1–190016-8; https://doi.org/10.1063/1.5067201
Published by AIP Publishing. 978-0-7354-1757-1/$30.00

sunshape. Several sunshape measurement methods have been developed recently [1-3]. Beside approaches using cameras and pyrheliometers with different apertures [1, 2] there are two methods that use Rotating Shadowband Irradiometers (RSI) [1, 3]. The method from [3] relies on a specially modified RSI that cannot be used for conventional DNI and GHI (Global Horizontal Irradiance) measurements. The RSI based method discussed here uses a conventional RSI without any hardware modification to enable sunshape measurements without affecting the RSIs fundamental function as a DNI measurement device. Thus, it allows to measure circumsolar radiation without any additional hardware.

After a short description of the method the validation results are shown followed by the results from the measurement campaigns at four sites in Spain, India and Morocco.

DESCRIPTION OF THE METHOD

The RSI method first derives the circumsolar contribution CSC(1°,3.2°). The CSC is defined as

$$CSC(\alpha_{in}, \alpha_{out}) = CSNI(\alpha_{in}, \alpha_{out}) / DNI(3.2°). \quad (1)$$

The CSC is the ratio of the circumsolar normal irradiance $CSNI(\alpha_{in}, \alpha_{out})$ received from angles between the inner angle α_{in} and the outer angle α_{out} from the center of the sun and $DNI(3.2°)$, the irradiance received from the total innermost 3.2° around the sun's center.

RSIs measure the GHI when the shadowband is resting below the RSI's pyranometer. After 30 seconds or one minute the shadowband is rotated around the pyranometer so that its shadow falls on the pyranometer. During the rotation of the shadowband, the pyranometer's irradiance signal is logged with high frequency. This signal is called burst and shown in Fig. 1. The burst is used in conventional RSIs to derive the diffuse horizontal irradiance (DHI) which is the minimum of the burst plus some diffuse irradiance blocked by the shadowband. From the GHI and DHI measurement the DNI is derived. In our case the burst is analyzed further in order to obtain the circumsolar horizontal irradiance and CSC as presented in [1]. A rough summary of the algorithm is illustrated in Fig. 2 which shows the 50 irradiance measurements centrically around the burst's minimum (also called well) together with intermediate results used to derive the CSC.

First, the minimum of the burst is located and the well is extracted from the burst. Then, the global horizontal irradiance (GHI) and the horizontal sky irradiance that is blocked by the shadowband I_{BSky} are derived. I_{BSky} does not contain circumsolar irradiance from the investigated angular intervals. I_{BSky} is read from 10 irradiance values taken from the outer parts of the well. The GHI is read from the outermost 10 values of the burst (5 on the left, 5 on the right) as in the common RSI evaluation.

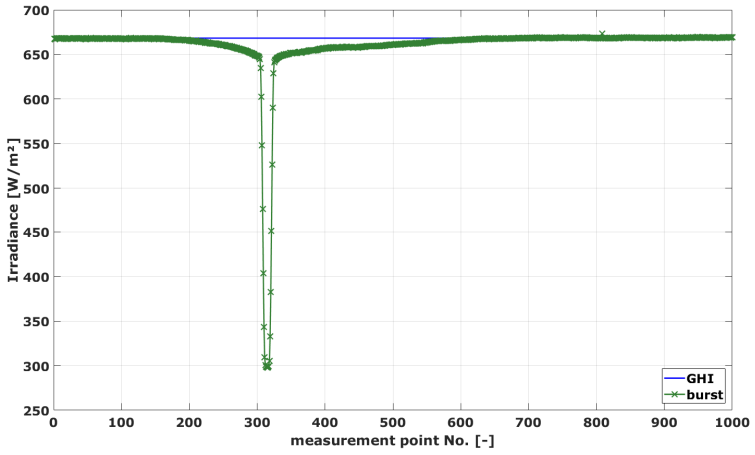

FIGURE 1. Irradiance signal logged during the rotation of the shadowband (also called burst) and derived irradiances for a measurement at PSA on September 11, 2011 14:47:00 (UTC)

For the further analysis the resolution of the well is increased by a factor of 10 using linear interpolation. The steep signal edges around the minimum are detected and linear regressions are performed. The point where these linear fits deviate by more than a given threshold from the well are detected as the innermost points of the circumsolar intervals (one left, one right of the minimum). These intervals have a certain width that is optimized for

each inner and outer angle of the CSC, e.g. α_{in}=1° and α_{out}=3.2°. The average irradiance in these intervals is the circumsolar indicator C_{ind}. Note that the circumsolar indicator has the units of an irradiance, but it is not the circumsolar irradiance, but just an intermediate result.

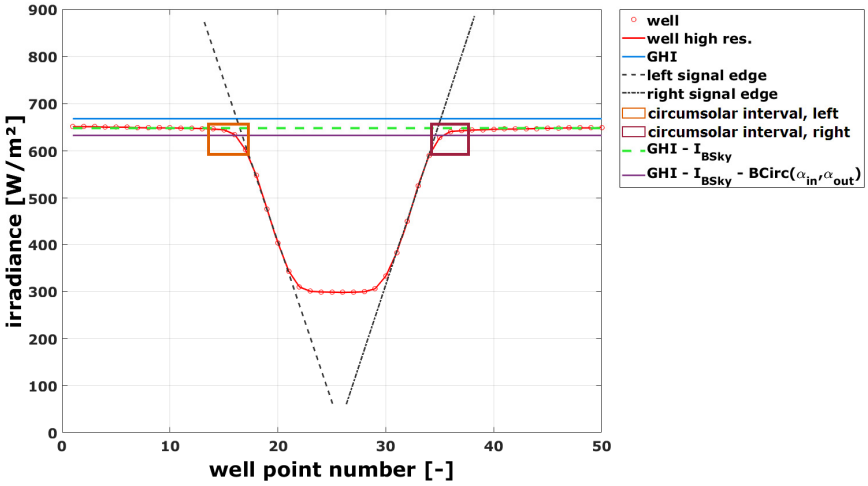

FIGURE 2. The central part of the burst (well) including parameters derived by the algorithm for the burst from Fig. 1. The actual irradiance measurements are shown as red circles (well) and an interpolation between these measurements as red solid line (well high resolution).

The blocked circumsolar horizontal irradiance is then calculated as

$$I_{BCirc}(\alpha_{in}, \alpha_{out}) = GHI - C_{ind}(\alpha_{in}, \alpha_{out}) - I_{BSky} \quad (2)$$

Then the preliminary or partial circumsolar contribution CSC_{part} is derived by dividing I_{BCirc} by the direct horizontal irradiance. The direct horizontal irradiance $DirHI$ is determined using the minimum of the well $I_{well,min}$ as

$$DirHI = GHI - I_{well,min} - I_{BSky} \quad (3)$$

As CSC_{part} only describes the part of the circumsolar radiation that is blocked by the shadowband, CSC_{part} is increased by a linear function to obtain the final CSC.

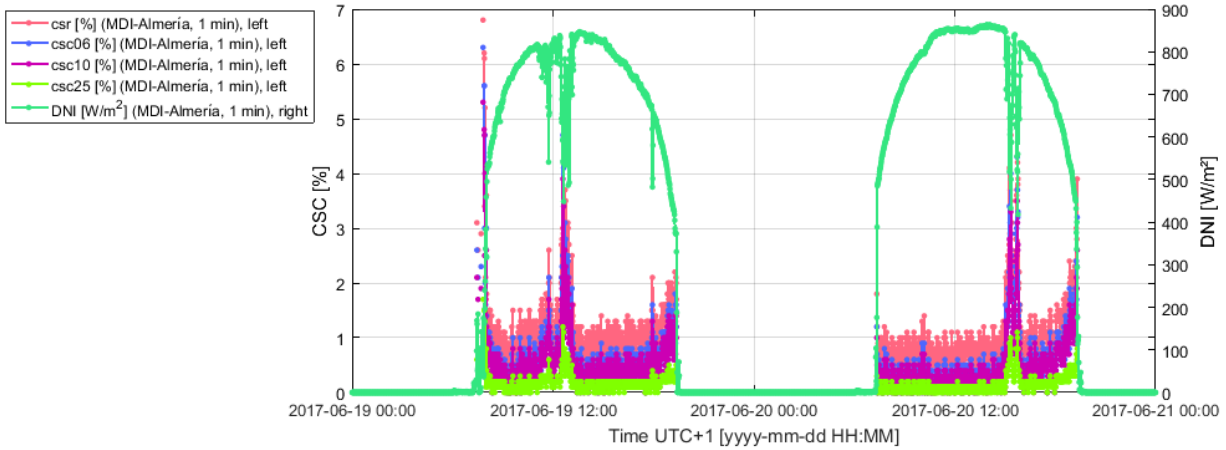

FIGURE 3. Visualization of automatically processed CSC values for several days of 2017 in the MDMS software.

For the exact selection of the position of the irradiance values used to determine I_{BCirc}, four constants *a, b, c* and *d* are needed. In addition, the slope *e* and the point of intersection *f* of the linear function converting CSC_{part} to the final CSC are required. The first four constants are determined by optimizing the Pearson correlation coefficient of CSC_{part} from the RSI and the CSC from a reference measurement (CSC_{ref}). The reference is provided by the SFERA

system [4]. The SFERA sunshape measurement system consists of Visidyne's Sun and Aureole Measurement instrument, a sun photometer and dedicated software. The two constants e and f of the linear function are then derived by linear regressions of CSC_{part} and CSC_{ref}. Every second month between April 2011 and December 2012 (both included) was used for the determination of these 6 constants.

The algorithm is implemented in our data management software MDMS (meteo data management software) and automatically processes and visualizes the received data. An example data set from a RSI in the city of Almería (36.836°N, -2.463°E, 23 m.a.m.s.l.) is shown in Fig. 3.

VALIDATION RESULTS AND CALIBRATION REQUIREMENTS

The method has been validated with sunshape data obtained with the SFERA sunshape measurement system at the Plataforma Solar de Almeria (PSA). Since the first validation from [1] that used 10 months of data and one RSI, the validation was enhanced to more than two years of validation, using data from three additional RSIs from Reichert GmbH and CSP Services GmbH. In Fig. 4 the CSC from the Twin-RSI 14.002.0013 and five months from PSA is shown in a 2D histogram as a function of the CSC from the reference system. The average of the RSI-derived CSC for bins of the reference values including the standard deviation and the RMSD are shown. The result indicates good agreement of the measurements with an underestimation of the RSI-derived values only at very high and less frequent CSC that occur only for low DNI. The median of the shown CSC of the reference system is 0.016, its mean is 0.046 and 90 % of the CSCs are below 0.112. The results from the other validation data sets are included in Table 1. The root mean square deviation (RMSD), bias, standard deviation (std) and the square of the Pearson correlation coefficient R^2 are shown next to the validation period. The RMSD and std are close to the exemplary median and about 30 % of the corresponding average. However, the median and the average are both small and hence the ratios of the RMSD and the std to the median and average are not relevant. The RMSD and std are much lower than 0.2 which is a quite frequent CSC. The bias is even lower than the RMSD and the std which indicates the good applicability to determine temporal averages of the CSC, e.g. over one year or a season. One can observe that all RSIs and data sets perform in a similar way with high R^2 and low error metrics. The data used to develop the algorithm was from RSP-4G1 and every second month from April 2011 to December 2012 (both included) and hence not overlapping with the validation data set.

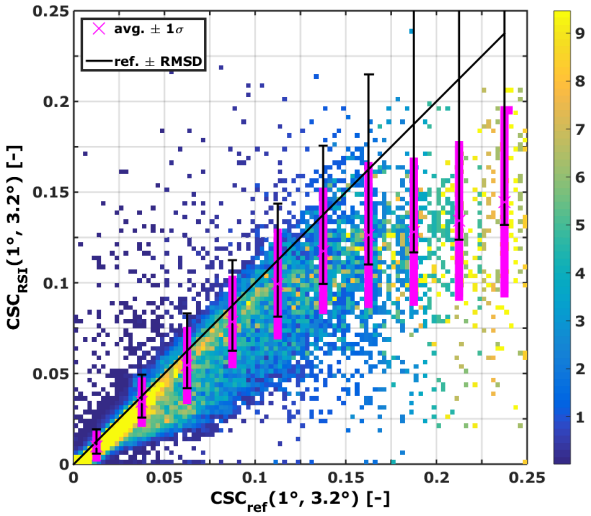

FIGURE 4. Comparison of the circumsolar contributions derived from the RSI1.1 and the reference instrument. The relative frequency is shown in percent of all results within each CSC_{ref} bin, so that also the much less frequent high CSC can be seen.

Within the validation also the calibration requirements were investigated. The applicability of non-instrument-specific calibration constants for the sunshape algorithm was studied. Note that we only refer to the constants a to f for the sunshape measurement here and not to the calibration constants required for DNI, GHI and the diffuse irradiance. The calibration constants for these standard irradiance measurements must of course be instrument specific and also a recalibration is required every two years [5, 6]. It was found that no individual sunshape

calibration is required for each instrument, but that the algorithm can be used with the same constants for all studied RSIs. The RMSD of CSC(1°,3.2°) measurements relative to the SFERA system only increased slightly from around 0.0138 to 0.0147 in average when the calibration constants from [1] were used as a generic set of calibration constants instead of an individual calibration. The comparison of these RMSDs is shown in Fig. 5 for three RSIs. This is a remarkable finding for the application of the algorithm, as virtually any Reichert GmbH and CSP Services GmbH RSI and even instruments that are already deployed in the field can now be used for sunshape measurements without an additional calibration or hardware modification. The method can also be adapted to RSIs from other manufacturers, but this has not been done so far. Only the signal logged during the rotation of the shadowband must be made available as a basis for the evaluation, which is achieved by simply changing the datalogger settings.

TABLE 1. Validation results obtained with four RSIs.

RSI name	Short name	Pyranometer serial number	Validation interval	RMSD	bias	std	R^2
4g0810	RSP-4G-1	PY57580	Every 2nd month starting with May 2011 to November 2012 (both incl.)	0.0158	0.0023	0.0157	0.8935
4g0918	RSP-4G-2	PY60281	April 27th - August 10th 2015	0.0153	0.0021	0.0152	0.8821
CSPS Twin RSI 14.002.0013	RSI1.1 RSI1.2	PY87337 PY87338	April 1st - August 10th 2015	0.0147 0.0161	-0.0045 -0.0048	0.0140 0.0153	0.9089 0.8903
CSPS Twin RSI 14.002.0014	RSI2.1 RSI2.2	PY87339 PY87340	April 1st - August 10th 2015	0.0140 0.0156	-0.0042 -0.0049	0.0133 0.0148	0.9174 0.8978

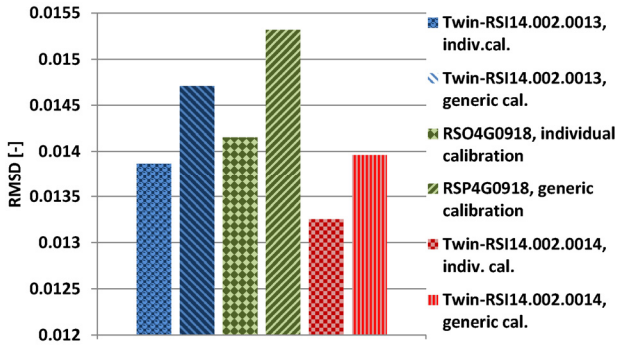

FIGURE 5. RMSDs of RSI based CSC measurements relative to the reference obtained with and without individual calibration of the RSI for the sunshape determination

DERIVING THE SUNSHAPE FROM CSC OR CSR

At times, not the CSC or CSR but the sunshape is required for the application of the circumsolar radiation data. In this case, a sunshape with the found CSC(1°,3.2°) can be derived directly using a look-up table in which the sunshapes' aureole power law slope and point of intersection are listed for each CSC(1°,3.2°). This sunshape can then be used in raytracing analyses or for the creation of a site specific average sunshape. The aureole L can be calculated with the angular distance from the center of the sun α as

$$L(\alpha) = e^{\kappa} \cdot \alpha^{\gamma}. \quad (4)$$

The sunshape within the solar disk is described using the Buie sunshape for this angular region. For cloudy situations, the parameters γ and κ for the aureole profile are obtained from the Buie model [7]. A flatter aureole slope derived from SFERA measurements at PSA is selected for aerosol dominated cases (Fig. 6). In this case, γ is -1.4296 for α in degree and only the point of intersection κ is varied according to CSC. Of course the slope of the aureole can also vary between different aerosol dominated cases. However, the deviation between slopes found for thin clouds and aerosols is much higher than the deviation between different observed aerosol cases.

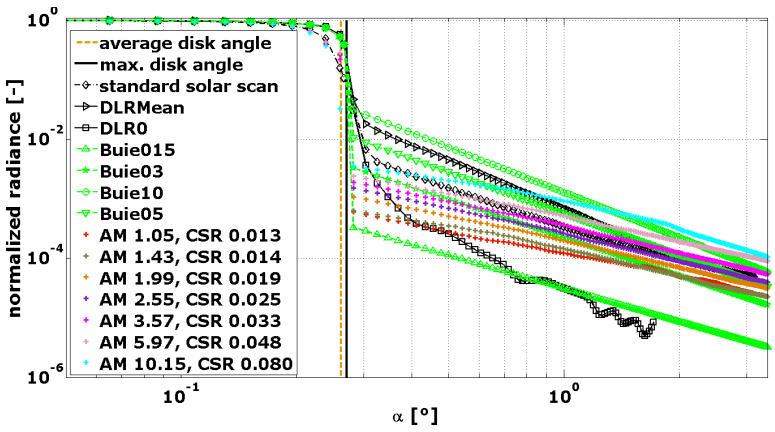

FIGURE 6. Aerosol sunshapes next to Buie sunshapes and other sunshapes from the literature. The slope of the aureole for AM1.99 is used for the creation of aerosol dominated sunshapes.

The Buie model is not used for the aerosol dominated cases as the Buie sunshapes are too steep for these situations. This is because clouds and aerosols were not treated separately for the determination of the Buie sunshapes, and because of the fitting methods used for their creation. Also most of the sunshapes with CSRs above approximately 5 % that were used by Buie for the creation of the model were measured in cloudy conditions. Further details on this issue of too steep Buie sunshapes for aerosols can be found in [1] and [8].

To identify cloudy time steps, a cloud detection algorithm can be applied using the Linke turbidity (TL) and a clear sky DNI. The TL coefficient represents the number of clean and dry atmospheres producing the observed extinction. Ineichen and Perez [9] present a formulation of TL to remove its original dependence on air mass. In the first step of the cloud detection, the TL of each timestamp and its temporal gradient is analyzed as described in [10] and [11]. The algorithm detects a cloud if an upper threshold for TL (calculated according to [9]) of 13 is exceeded or if the TL displays a strong temporal variability (more than 0.06 difference between two time steps of 1 min). The threshold should be adapted to the site of interest to reach the highest possible accuracy. In a second step the DNI is compared to a clear sky DNI derived from the lowest TL found for the investigated day and timestamps which were not detected as cloudy in the first step. If only cloudy DNIs were found in the first step of the algorithm, the average of the clear sky TL found from the previous non cloudy days is used. If the DNI for a timestamp is more than X % lower than the clear sky DNI, the timestamp is interpreted as cloudy. The threshold X is variable and depends linearly on the AM. At solar noon, deviations of more than 10 % are considered as cloudy, where at sun rise deviations have to reach 30 %.

In selected cases a specific type of sunshape is implemented in the plant performance model and only the CSR is handed over to the model to select the sunshape from a set of these predefined sunshapes. Such sunshapes can be for example a set of Buie sunshapes with CSRs of 0.01 to 1 in steps of 0.01. Also in these cases the CSC can be translated to the required information using a look up table in which the CSRs and the corresponding CSC(1°,3.2°) for the Buie sunshapes are saved.

RESULTS FROM THE MEASUREMENT CAMPAIGNS AT FOUR SITES IN SPAIN, INDIA AND MOROCCO

The algorithm was used at four sites to gather in total over four years of circumsolar radiation data. The coordinates and the evaluation interval presented in this work are given in Table 2. All four stations are still in operation. More details on the stations can be found in [12] and [13]. The histograms of all four sites are shown in Fig. 7. While the histograms for PSA, Erfoud and Zagora are similar to each other, the histogram for Greater Noida deviates strongly with more frequent higher CSR. This fits to the expectation as high turbidities prevail in Greater Noida. The histogram from Greater Noida is similar to data found for Masdar, UAE as presented in [1]. Note that a small deviation can also be caused by seasonal effects which are not considered here, although methods for their removal exist [1].

The histograms of the datasets from PSA obtained with RSP-4G1 and the SFERA reference system are shown in Fig. 8. Good agreement of the histograms can be observed. Slightly less cases of the first bin are found, slightly

more cases in the second bin. The difference between the RSI and the reference histograms is much smaller than the deviation of the histograms for hazy and rather clear sites (e.g. Greater Noida and PSA). Such deviations between different sites of interest can be distinguished well by the RSI based measurements.

TABLE 2. Coordinates of investigated sites, and evaluated interval.

Site name	Latitude [°N]	Longitude [°E]	Altitude [m.a.m.s.l.]	Evaluation interval
Plataforma Solar de Almería, Spain	37.09	-2.36	500	Every 2nd month starting with May 2011 to November 2012 (both incl.)
Erfoud, Morocco	31.49	-4.22	859	04/2016 – 03/2017
Zagora, Morocco	30.27	-5.85	783	04/2016, 05/2016 – 11/2016, 11/2016 – 03/2017
Greater Noida, NETRA, India	28.50	77.47	195	01/2017 – 06/2017

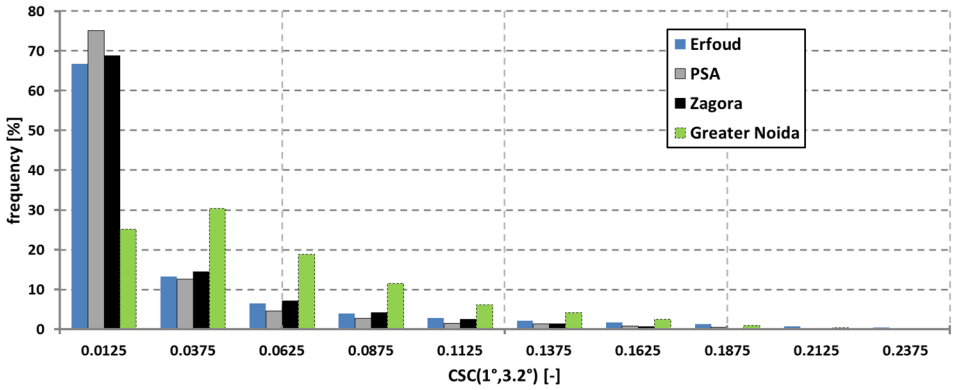

FIGURE 7. Histograms of CSC from the four sites. All data from the given intervals with DNIs above 150 W/m², GHIs above 10 W/m² and solar elevation angles above 5° are shown.

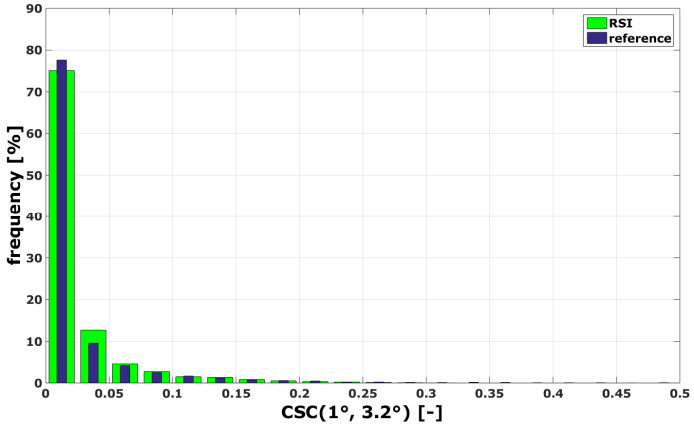

FIGURE 8. Histograms of CSC from the RSI-4G1 and the SFERA reference system from PSA. All data from the test period with DNIs above 150 W/m², GHIs above 10 W/m² and solar elevation angles above 5° are shown.

CONCLUSIONS

The presented RSI-based sunshape measurement algorithm has been validated with four RSIs and more than two years of data. It was found that no individual calibration is required per instrument and the algorithm has been implemented for automatic data processing, so that common RSI stations can be used to measure the sunshape with

comparably low extra effort. A method to derive sunshapes from the CSC measurements was developed and presented. The RSI method is demonstrated at four sites in Morocco, India and Spain. While the three sites in Morocco and Spain showed similar histograms of the CSC, the data from India (Greater Noida) was characterized by significantly more frequent high CSC. This RSI-based method has significantly lower maintenance effort, less data gaps and lower instrument cost compared to other sunshape measurement systems. Therefore, it is now possible to include circumsolar radiation measurements in standard solar resource assessment campaigns without the need for additional hardware.

ACKNOWLEDGMENTS

We thank the Helmholtz Association for partly funding the research related to the method development and the stations in Morocco and Spain within the Desergy project. We thank the KfW for funding the work related to the station in India within the NETRA CST project.

REFERENCES

1. Wilbert, S.: Determination of Circumsolar Radiation and its Effect on Concentrating Solar Power. PhD thesis, RWTH Aachen, DLR, http://darwin.bth.rwth-aachen.de/opus3/volltexte/2014/5171/ (2014).
2. Kalapatapu, R., M. Chiesa, P. Armstrong, and S. Wilbert. 2012. Measurement of DNI Angular Distribution with a Sunshape Profiling Irradiometer. SolarPACES 2012, at Marrakesh, Morocco.
3. Schrott, S, T. Schmidt, T. Hornung, P. Nitz. 2014. Scientific system for high-resolution measurement of the circumsolar radiation. AIP Conference Proceedings 1616, 88 (2014); doi: http://dx.doi.org/10.1063/1.4897035.
4. Wilbert, S., B. Reinhardt, J. DeVore, M. Röger, R. Pitz-Paal, C. Gueymard, and R. Buras. 2013. Measurement of Solar Radiance Profiles With the Sun and Aureole Measurement System. Journal of Solar Energy Engineering no. 135 (4):041002-041002. doi: http://dx.doi.org/10.1115/1.4024244.
5. Jessen, W., S. Wilbert, B. Nouri, N. Geuder, and H. Fritz. 2016. "Calibration methods for rotating shadowband irradiometers and optimizing the calibration duration." Atmos. Meas. Tech. no. 9 (4):1601-1612. doi: http://dx.doi.org/10.5194/amt-9-1601-2016.
6. Geuder, N, R Affolter, B Kraas, and S Wilbert. 2014. "Long-term Behavior, Accuracy and Drift of LI-200 Pyranometers as Radiation Sensors in Rotating Shadowband Irradiometers (RSI)." Energy Procedia no. 49:2330-2339. https://doi.org/10.1016/j.egypro.2014.03.247
7. D. Buie, A. Monger, and C. Dey. Sunshape distributions for terrestrial solar simulations. Solar Energy, 74(2):113 122, 2003b.
8. Wilbert, Stefan, Robert Pitz-Paal, and Joachim Jaus. 2013. "Comparison of measurement techniques for the determination of circumsolar irradiance." AIP Conference Proceedings no. 1556 (1):162-167. doi: http://dx.doi.org/10.1063/1.4822222.
9. Ineichen, Pierre, and Richard Perez. 2002. "A new airmass independent formulation for the Linke turbidity coefficient." Solar Energy no. 73 (3):151-157.
10. Wilbert, Stefan, Stefan Kleindiek, Bijan Nouri, Norbert Geuder, Aron Habte, Marko Schwandt, and Frank Vignola. 2016. "Uncertainty of rotating shadowband irradiometers and Si-pyranometers including the spectral irradiance error." AIP Conference Proceedings no. 1734 (1):150009. doi: http://dx.doi.org/10.1063/1.4949241.
11. Hanrieder, Natalie, M. Sengupta, Yu Xie, Stefan Wilbert, and Robert Pitz-Paal. 2016. "Modeling beam attenuation in solar tower plants using common DNI measurements." Solar Energy no. 129:244-255. doi: https://doi.org/10.1016/j.solener.2016.01.051.
12. Pozo-Vázquez, D., S. Wilbert, C. Gueymard, L. Alados-Arboledas, F. J. Santos-Alamillos, and M.J. Granados-Muñoz. 2011. Interannual Variability of Long Time Series of DNI and GHI at PSA, Spain. Paper read at SolarPACES Conference, at Granada, Spain.
13. Schüler, D., S. Wilbert, N. Geuder, R. Affolter, F. Wolfertstetter, C. Prahl, M. Röger, M. Schroedter-Homscheidt, G. Abdellatif, A. Allah Guizani, M. Balghouthi, A. Khalil, A. Mezrhab, A. Al-Salaymeh, N. Yassaa, F. Chellali, D. Draou, P. Blanc, J. Dubranna, and O. M. K. Sabry. 2016. "The enerMENA meteorological network – Solar radiation measurements in the MENA region." AIP Conference Proceedings no. 1734 (1):150008. doi: http://dx.doi.org/10.1063/1.4949240.